ORIGINAL RESEARCH

Bioactive Porous Composite Implant Guides Mesenchymal Stem Cell Differentiation and Migration to Accelerate Bone Reconstruction

Sheng Wang[1,*], Demeng Xia [2,3,*], Wenxue Dou[4,*], Aimin Chen[1], Shuogui Xu [2]

[1]Department of Traumatic Orthopedics, Shanghai Fourth People's Hospital, School of Medicine, Tongji University, Shanghai, 200434, People's Republic of China; [2]Department of Traumatic Orthopedics, Changhai Hospital, Naval Medical University, Shanghai, 200433, People's Republic of China; [3]Department of Clinical Medicine, Hainan Health Vocational College, Haikou, 570100, People's Republic of China; [4]Department of Stomatology, Shanghai East Hospital, Tongji University, Shanghai, 200120, People's Republic of China

*These authors contributed equally to this work

Correspondence: Shuogui Xu, Department of Emergency, Changhai Hospital, Naval Medical University, Xiangyin Road, Shanghai, 200433, People's Republic of China, Email 18516116672@163.com; Aimin Chen, Department of traumatic orthopedics, Shanghai Fourth People's Hospital, School of Medicine, Tongji University, Shanghai, 200434, People's Republic of China, Email chenaimin2023@163.com

Background: Delayed healing and non-healing of bone defects pose significant challenges in clinical practice, with metal materials increasingly recognized for their significance in addressing these issues. Among these materials, Strontium (Sr) and Zinc (Zn) have emerged as promising agents for promoting bone repair. Building upon this insight, this research evaluates the impact of a porous $Sr@Zn@SiO_2$ nanocomposite implant on bone regeneration, aiming to advance the field of bone repair.

Methods: The preparation of the $Sr@Zn@SiO_2$ composite implant involves various techniques such as roasting, centrifugation, and washing. The material's composition is examined, and its microstructure and element distribution are analyzed using TEM and elemental scanning technology. In vitro experiments entail the isolation and characterization of BMSCs followed by safety assessments of the implant material, evaluation of cell migration capabilities, and relevant proliferation markers. Mechanistically, this study delves into key targets associated with significant changes in the osteogenic process. In vivo experiments involve establishing a rat femur bone defect model, followed by assessment of the osteogenic potential of $Sr@Zn@SiO_2$ using Micro-CT imaging and tissue section staining.

Results: Through in vivo and in vitro investigations, we validate the osteogenic efficacy of the $Sr@Zn@SiO_2$ composite implant. In vitro analyses demonstrate that porous $Sr@Zn@SiO_2$ nanocomposite materials upregulate BMP-2 expression, leading to the activation of Smad1/5/9 phosphorylation and subsequent activation of downstream osteogenic genes, culminating in BMSCs osteogenic differentiation and bone proliferation. And the migration of BMSCs is closely related to the high expression of CXCL12/CXCR4, which will also provide the conditions for osteogenesis. In vivo, the osteogenic ability of $Sr@Zn@SiO_2$ was also confirmed in rats.

Conclusion: In our research, the porous $Sr@Zn@SiO_2$ composite implant displays prominent osteogenic effect and promotes the migration and differentiation of BMSCs to promote bone defect healing. This bioactive implant has surgical application potential in the future.

Keywords: bioactive porous composite, differentiation and migration, bone reconstruction, smad1/5/9

Introduction

Bone defects represent a significant challenge for orthopedic practitioners, and there are various reasons for the occurrence of bone defects.[1] Though bone tissue possesses a robust capacity for regeneration, approximately 10% of fracture patients experience healing complications, such as delays or non-union, resulting in severe implications for their well-being.[2] As research advances, the therapeutic potential of bone marrow mesenchymal stem cells (BMSCs) becomes increasingly clear, with their pivotal roles in intramembranous ossification, endochondral ossification, and bone

12111

Graphical Abstract
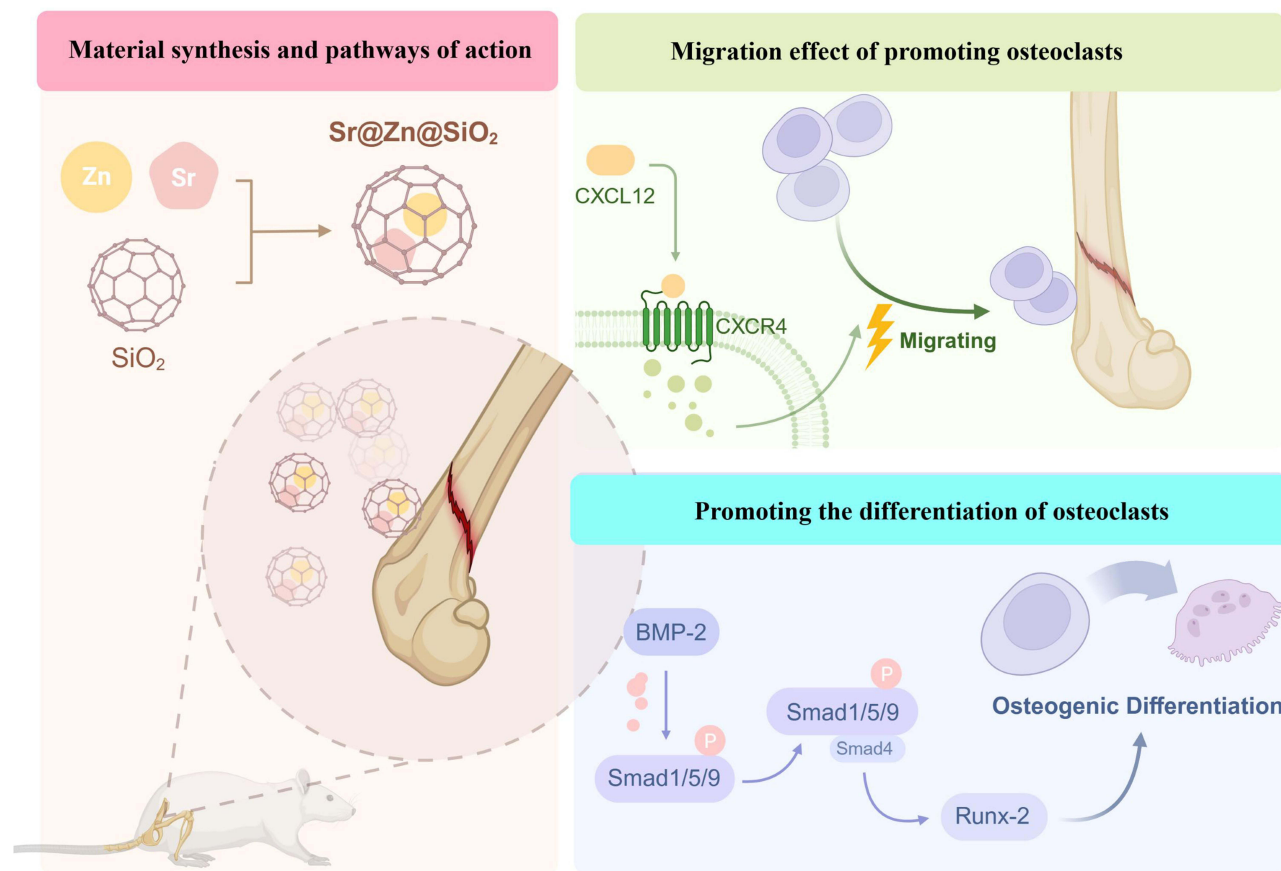
maintenance.[3,4] Therefore, the urgent question facing us is how to effectively activate and direct the growth and differentiation of these cells.

In medicine, the broader application of metal elements is gaining traction, particularly certain trace metals that have demonstrated their potency in enhancing cell proliferation, differentiation,[5] immunomodulation[6] and providing antibacterial effects.[7,8] These properties lay the groundwork for metal utilization in biological applications.

As an essential trace element for human body, Sr is an important part of human skeleton. The function and structure of blood vessels are closely related to Sr. At the same time, Sr plays a role in maintaining electrolyte balance in terms of physiological function. Sr also plays an important role in preventing cardiovascular diseases such as coronary heart disease and hypertension, treating dental caries and alleviating diabetes.[9] More importantly, Sr can promote bone growth and development, prevent and treat osteoporosis. The drug strontium ranelate has been widely used in the treatment of osteoporosis.[10] Zinc is also an essential trace element in the human body, with important physiological functions and a wide range of pharmacological effects. Zn can participate in enzyme synthesis and activation, promoting growth, development, and wound healing. Meanwhile, Zn has a clear ability to form blood vessels, which is closely related to its promotion of repair function.[11] Zn also has antibacterial effects and has been widely used in the treatment of infections. In recent years, studies have shown that zinc has a strong regulatory effect on alkaline phosphatase activity and has the potential for osteogenesis.[12]

Various materials have been used as drug carriers in recent years. Electrospun nanofiber scaffolds can mimic the body's natural extracellular matrix (ECM) in morphology and structure, which is beneficial for cell adhesion and proliferation, the invention can create favorable conditions for the regeneration of tissues and organs.[13] Hydrogel is

a kind of water-absorbent material, and it has been used in biomedicine field in recent years.[14] Among them, nano-composite hydrogel can sense pressure. We chose the silicon dioxide as a slow-release drug that can be released slowly to achieve therapeutic effects.[15]

SiO$_2$ nanomaterials do not have significant osteogenic ability, but they are an extremely excellent carrier in the biomedical field. Their inherent pore structure provides sustained release characteristics, which helps slow release of drugs or materials loaded in them.[16] Researches have shown that they can encapsulate Se elements and promote fracture healing.[5] Similarly, SiO$_2$ loaded with BMP-2 also exhibits osteogenic ability.[17] Therefore, we believe that SiO$_2$ is an excellent choice for carrier materials.

Furthermore, Sr is known for its vasogenic effects, while Zn can mitigate infection risks.[18] In light of these findings, we have engineered a novel Sr@Zn@SiO$_2$ nano-composite material using nano-encapsulation technologies, which facilitates bone growth by steadily releasing the incorporated metals. However, a large amount of metals implanted at one time may cause toxic damage to the human body, and nano-level SiO$_2$ is a loading agent with slow releasing effect, which can safely and stably wrap metals and release them.[19] In light of these findings, we have engineered a novel Sr@Zn@SiO$_2$ nano-composite material using nano-encapsulation technologies, which facilitates bone growth by steadily releasing the incorporated metals.

The clinical application of bioactive materials requires various evaluations.[20] Based on this fact, we tested the basic element distribution and cell safety of the material. Then, we verified the osteogenic ability of the material, we conducted cell verification firstly. BMSCs are the key cells for osteogenesis, and promoting their migration and differentiation is a research focus. In our preclinical research, it is not only satisfied with the phenomenon of osteogenesis of this material, but more importantly to explore its internal mechanism if we want to make this material in clinical application. Based on this, we have carried out research in this aspect. Transwell migration assay confirmed that Sr@Zn@SiO$_2$ can promote migration of BMSCs. Meanwhile, Under the influence of the Sr@Zn@SiO$_2$, we detected increased expression of CXCL12 and its unique receptor CXCR4, which are associated with migration ability, and the CXCL12/CXCR4 axis is critical for the migration ability of BMSCs.[21] Through the activity of alkaline phosphatase and the results of staining with alizarin red staining, we were surprised to find the ability of the material in osteogenesis. In terms of osteogenic markers, previous studies have confirmed that Runx2 is a transcription factor that plays an important role in osteogenic differentiation, BMP-2 can accelerate the phosphorylation of Smad1, Smad5 and Smad9, so that phosphorylated Smad1/5/9 can form a complex with Smad 4. This complex can interact with Runx2 in the nucleus to facilitate the smooth process of osteogenesis,[22] and changes in the expression of downstream osteogenic gene OSX also provide basis for osteogenesis.[23]

In vivo, the rat femur bone defect model serves as the objective. Using Micro-CT assessments and toluidine blue staining, we can comprehensively gauge the osteogenic efficacy of our materials. This study aims to set the stage for the subsequent adoption of the Sr@Zn@SiO$_2$ nano-composite. We also anticipate that these findings will inform the application of metal materials in treating bone defects more broadly.

Methods
Synthesis and Characterization of Porous Sr@Zn@SiO$_2$ Nanocomposite Implant

According to previous experience in successful synthesis of silica materials,[24,25] firstly, CTAB and ethylene glycol were dissolved in deionized water. Then stirring at 50°C alkaline condition for 15 minutes, adding TEOS, centrifuging, washing and then roasting at 550°C Muffle furnace for 6 hours. Mesoporous silica can be obtained. Then Silica was combined with materials Zinc chloride and strontium chloride, stirred with an aqueous solution of PVP for 30 minutes under alkaline conditions, placed in 50mL polytetrafluoroethylene lining, and reacted in a reactor at 140°C for 2 hours. After the reaction, zinc chloride and strontium chloride will exist in the form of oxides, the oxide form slows the release of the element. After centrifugal washing, the Sr@Zn@SiO$_2$ nanocomposite implant can be obtained. TEM and element scanning techniques were used to observe the microstructure and element distribution of the materials. The specific surface area and pore volume of the products were measured by the Brunauer–Emmett–Teller (BET) and Barrett–Joyner–Halenda (BJH) methods (Quantachrome, Autosorb-1MP).

Sr@Zn@SiO$_2$ Nanocomposite Release Kinetics

We detected the cumulative release kinetics of Sr and Zn from the porous Sr@Zn@SiO$_2$ nanocomposites when the pH of PBS solution is 7.35 and the temperature is 37°C. 6 milligrams of the porous Sr@Zn@SiO$_2$ nanocomposites was dispersed with ultrasonication in 6 mL of PBS. They were incubated for 12, 24, 48, 96 and 168 hours respectively, and centrifuged at each time point. 6 mL of supernatant was removed, and the same volume of PBS buffer was added to continue shaking. The contents of released Sr and Zn were determined according to inductively coupled plasma optical emission spectrometer (ICP-OES), then calculated release ratio.

Animal and Cell Culture

All experiments were approved by the Laboratory Animal Center of the Naval Medical University. The work followed ARRIVE guidelines (Animals in Research: Reporting in Vivo Experiments).[26] 78 SD rats (six-week-old, male) with an average body weight of about 250g were from Shanghai Sipple-BiKai Laboratory Animal Company. These rats are raised by the Laboratory Animal Center of the Naval Medical University. All animal studies were maintained in accordance with the Guideline for ethical review of animal welfare of laboratory animals published by the China National Standardization Management Committee (publication No. GB/T 35892–2018). Animal feeding adopts 12-hours rotation of day and night lighting, the temperature is controlled at about 23°C, the relative humidity is about 50%, and the animals are free to eat and drink during feeding.

The study began after the rats were fed for one week. BMSCs were isolated from the medullary cavity of the femur of SD rats. Cells were then cultured in rat BMSCs complete culture medium in a 5% CO$_2$ incubator at 37°C. The cultured cells were placed under the microscope for observation. The results indicated that the observed cells were adherent cells. The medium was changed every 3 days, and 3—4 generations of BMSCs were used for follow-up experiments.

Biosafety Assessment on Sr@Zn@SiO$_2$ Nanocomposite Implant

Cell Safety Verification

In vitro safety of porous Sr@Zn@SiO$_2$ nanocomposite implant was evaluated by measuring their inhibitory effect on the BMSCs proliferation. BMSCs were inoculated into 96-well plates at 37°C, 5% CO$_2$, and incubated for 24 hours. After 24 hours, the incubation cells were increased with the concentration of Sr@Zn@SiO$_2$ nanocomposite implant (0—400μg/mL). On the second day, the cell proliferation was detected by CCK-8 assay. The absorbance of 450nm wavelength was selected as the detection index, and the measurement was carried out with the enzyme marker to observe if the cells' activity was affected by the material.

Animal Safety Verification

Six male SD rats were randomly divided into 2 groups with 3 rats in each group to create a femur defect model (see 2.10 for specific steps). The defect in the blank group was not filled with material, while the defect in the experimental group was filled with Sr@Zn@SiO$_2$. Blood routine and blood biochemical results were measured 7 and 14 days after the operation, and the rats were killed 14 days later, and the heart, liver, kidney, lung and spleen of the rats were taken for HE staining, the results of experimental group and blank group were compared.

Evaluation of in vitro Cell Migration

BMSCs were divided into 3 groups. Group A was a blank group without any material in the culture medium. 400μg/mL SiO$_2$ was added into the culture medium of group B as the control group. The 400μg/mL Sr@Zn@SiO$_2$ was added into the culture medium of group C as the material group. The cell serum starvation model was established to wash, resuspend and dilute the cells after trypsin digestion. Finally, crystal violet solution was added to stain the samples, and the samples were observed under a microscope, the magnification was adjusted, and the number of cells in the visual field was recorded. WB and PCR were performed for CXCR4 in the above three groups of cells, and Elisa was performed for CXCL12, which are used to judge the strength cell migration ability.

Expression of Osteogenic Related Markers

Determination of Alizarin Red Staining

The BMSCs were inoculated on the material, blank and control groups for culture. After the experimental process of rinsing, fixing and washing the medium 14 days later, 1mL alizarin red dye solution was added into the corresponding holes of the three groups for incubation and observation under the microscope.

Determination of Alkaline Phosphatase

The BMSCs were inoculated on material, blank and control groups and cultured for 7 days. After cleaning, fixing and re-cleaning, and repeated freeze-thaw centrifugation at low temperature, the reaction was terminated after the obtained supernatant was fully mixed with nitrophenol phosphate solution. The sample was transferred to a 96-well plate to measure the absorbance of the sample at different wavelengths (OD562). Ratios were calculated to compare the relative activity of ALP among the three groups.

For the Determination of Osteogenic Gene Expression, See Below

Western Blot

BMSCs were coated in 6-well plates with the concentration of 2×10^4 cells/cm^2 and divided into material group, blank group and control group. 7 days after osteogenic induction, BMSCs were washed 3 times with PBS to prepare gel, and then samples were taken, electrophoresis, membrane transfer, protein detection, membrane sealing, antibody incubation and color development were performed. This part was mainly used to detect the protein expression levels of CXCR4, Smad1/5/9 and p-Smad1/5/9 involved in the study.

Polymerase Chain Reaction

BMSCs with 2×10^4 cells/cm^2 concentration were divided into material group, blank group and control group. After 7 days of osteogenic induction, the transcriptional levels of osteogenic differentiation related genes Runx2, OCN, BMP-2 and Smad1 were evaluated. We used standard primers. Total cell RNA was extracted according to the instructions. After PCR amplification, the relative transcription level was calculated.

Enzyme Linked Immunosorbent Assay

In this part, we mainly performed Elisa detection on CXCL12. The standard product, standard product and sample diluent and the sample to be tested were added to the hole with 100μL each, and recorded as the standard hole, blank hole and sample hole respectively. Then, the CXCL12 was coated and incubated for 90 minutes. After adding biotinylated antibody working solution of 100μL, incubate again for 60 minutes, remove the liquid for washing, soaking, patting dry and other operations, then add enzyme binding working solution of 100μL to each hole, and incubate at 37°C after coating. Until the gradient appears, the (OD value) of each hole is measured at 450nm wavelength.

Immunofluorescence Test

BMSCs of 2×10^4 cells/cm^2 were taken, fixed with 4% paraformaldehyde for 20 minutes, washed for 3 times, incubated on ice for 2 minutes, and washed with PBS for 3 times again. Rabbit serum diluted with buffer solution was incubated for 1 hour, then primary antibody (1:100) was added overnight at 4°C, and after washing, secondary antibody was added and incubated for 1 hour away from light at room temperature. After staining the nuclei for 15minutes, the cells were observed under a fluorescence microscope using 20ul anti-fluorescence quencher.

Establishment of Bone Defect Model and Material Filling in Rats

The 72 male SD rats were randomly divided into 3 groups with 24 rats each. They were labeled as material group (Sr@Zn@SiO$_2$), control group (SiO$_2$ group) and blank group (no materials added). All rats were anesthesia with isoflurane. The head and limbs were fixed behind the operating table, and a longitudinal incision about 3—5cm long was made in the middle part of the left femur after hair removal, disinfection, and towel covering. The skin, muscle and

other tissues were gradually separated, the supracondylar position of the femur was found, the periost was fully detached, and a hollow electric drill with a diameter of 2mm was used to drill holes with a depth of 5mm. The bone defects were filled with materials respectively, and the skin incisions were sutured and disinfected, and gentamicin was injected intraperitoneally to prevent infection. The rats were returned to the cage for 4 weeks, 12 rats were killed in each group. After separating the rat femur, the rat femur was stained with toluidine blue, and 3D reconstruction was performed using Micro-CT scanning and CT-Vox software. After reconstruction, relevant parameters of bone regeneration were calculated.

Statistic Analysis

All experiments were performed at least three times. Results were represented by mean ± standard deviation, and statistical pictures were drawn by GraphPad Prism. Statistical analysis was performed by SPSS software. The two groups of data met the criteria of normal distribution and homogeneity of variance, and T-test was used. Multiple groups of data meet the criteria of normal distribution and homogeneity of variance, and analysis of variance is used. $P<0.05$ was statistically significant (*$P <0.05$, **$P < 0.01$, ***$P < 0.001$).

Results

Synthesis and Characterization of Porous Sr@Zn@SiO$_2$ Nanocomposite Implant

The microstructure of Sr@Zn@SiO$_2$ at 200nm, 100nm, and 20nm was observed by TEM technique (Figure 1A). Element scanning experiments were conducted to verify the uniform distribution of Sr, Zn, Si and O elements in the material (different colors represent different distributions), and the four elements were evenly distributed in the material (Figure 1B). The successful synthesis of Sr@Zn@SiO$_2$ nanocomposite implant was confirmed.

Sr@Zn@SiO$_2$ Nanocomposite Release Kinetics and Pore Size Distribution

The release of Sr and Zn was measured under normal physiological conditions. The release rate of Sr and Zn gradually increased in the first 96 hours, and reached the peak at 96 hours, stable release in the following time (Figure 1C), and achieved the intended slow release. N$_2$ adsorption/desorption isotherms and pore size distribution of Sr@Zn@SiO$_2$ had been tested (Figure 1D and E).

Culture of BMSCs

After 3—4 generations of BMSCs culture, we detected the positive rate of cell surface markers, indicating that the positive rate of CD11b was 1.76%, that of CD45 was 2.05%, that of CD44 was 99%, and that of CD90 was 98.6% (Figure 2A). The successful isolation of BMSCs was confirmed.

Validation of Sr@Zn@SiO$_2$ Safety

The isolated BMSCs were added with the concentrations of Sr@Zn@SiO2 at 0μg/mL, 25μg/mL, 50μg/mL, 100μg/mL, 200μg/mL and 400μg/mL, respectively, and the cell activity was measured after 0, 12, 24 and 48 hours, and there was no effect on the activity of BMSCs in Sr@Zn@SiO$_2$ material with 0—400μg/mL concentration (Figure 2B). At the same time, we co-cultured BMSCs with 400μg/mL concentration of materials (material group), the same concentration of SiO$_2$ (control group) and blank control group (blank group) for 24 hours to observe the spread morphology of BMSCs, and the results are as follows (Figure 2C). It was proved that the material had no significant effect on the activity of rat BMSCs.

At the same time, we conducted an experiment on the safety of the material in rats. The rats were killed on the 14th day after the defect filling was completed, and the heart, liver, kidney, spleen and lung of the rats were taken for HE staining (Figure 3A). Blood routine and blood biochemical results were measured 7 and 14 days later, including red blood cells, white blood cells, platelets and urea nitrogen. ALT, AST (Figure 3B and C), the results indicated that there was no statistical difference between the blank group and the experimental group. This confirmed that Sr@Zn@SiO$_2$ was no significant effect on blood routine, liver and kidney function and vital organ.
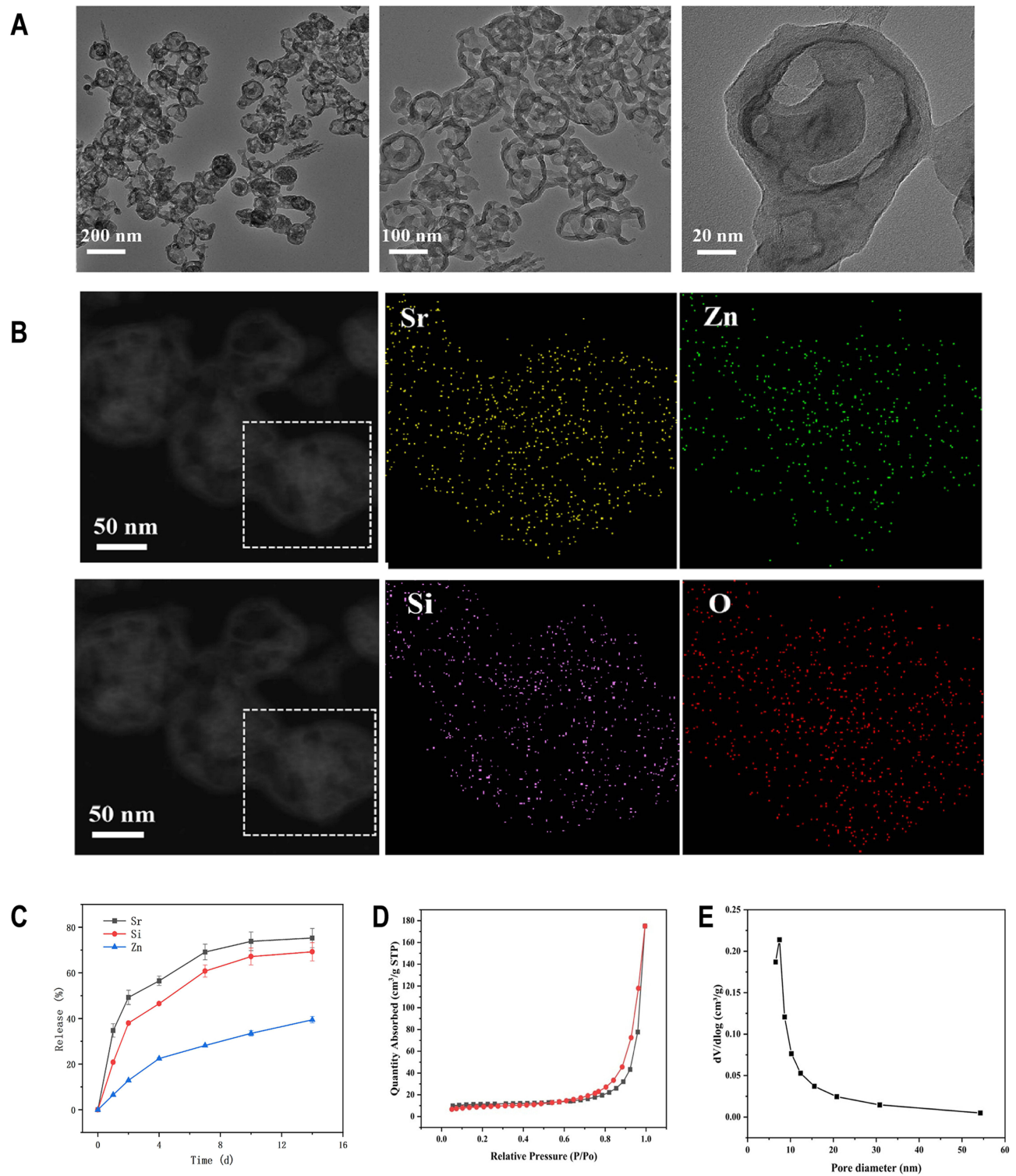
Figure 1 Characterization of Sr@Zn@SiO$_2$ and release kinetics. (**A**) TEM micrographs at 200nm, 100nm and 20nm under the microscope. (**B**) Scanning distribution diagram of Sr, Zn, Si and O elements. (**C**) The release kinetics of Sr and Zn. (**D**) N$_2$ adsorption/desorption isotherms. (**E**) pore size distribution of Sr@Zn@SiO$_2$.

Sr@Zn@SiO$_2$ Promoted the Migration of BMSCs

BMSCs were mixed with 400μg/mL concentration material as the material group, mixed with the same concentration of SiO$_2$ as the control group, and no material was added as the blank group (Hereinafter referred to as material group, control group and blank group respectively). After culture at 37°C for 7 days, the number of invasive cells in each group
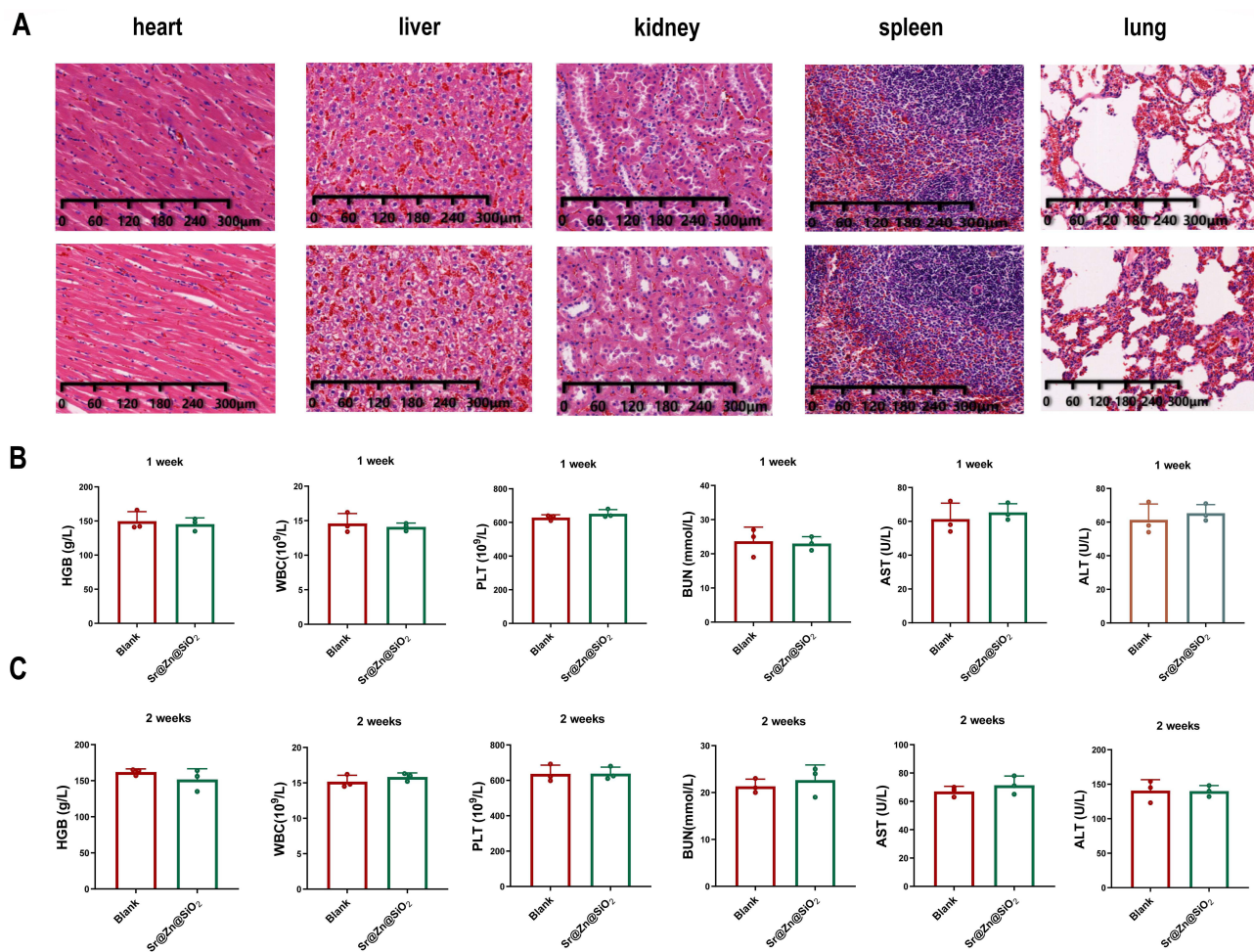
Figure 2 Screening of BMSCs and determination of material safety in vitro and in vivo. (**A**) The positive rate of cell surface markers, 1.76% for CD11b, 2.05% for CD45, 99.0% for CD44 and 98.6% for CD90. (**B**) Cell activity under different concentrations of Sr@Zn@SiO$_2$ (from left to right are 0, 12, 24 and 48 hours). (**C**) Spread morphology of MSCs after co-culture with materials, blank materials and 24 hours alone culture.

was amplified 100 times, Transwell's imaging results also indicated that the number of invasive cells in the material group was significantly higher than in the other groups (Figure 4A-C). Based on this, we also explored the mechanism. The results of Western blot experiment indicated that there was no significant difference in the expression of CXCR4 protein between the blank group and the control group, while the expression of CXCR4 protein in the material group was significantly increased (Figure 4D and E). The experimental results of the same PCR suggested that there were also differences in CXCR4 gene expression between the material group and the blank group (Figure 4F). Elisa results indicated that CXCL12 expression in the material group was significantly higher than that in the control group and the blank group (Figure 4G). This validated the material's ability to promote BMSCs migration.

Sr@Zn@SiO$_2$ Promoted the Osteogenic Differentiation of BMSCs

After 7 days of osteogenic induction, the activity of ALP was measured by biochemical methods and the amount of calcium deposition was significantly increased. In terms of ALP activity, there was a statistical difference between the cultured material group and the blank group (Figure 4H). After 1 and 7 days of osteogenic induction, the amount of calcium deposition was measured by alizarin red staining, after alizarin red staining, it was found that the amount of calcium deposition in the blank group and the control group had no significant change, while the red deposition in the material group was more obvious, the results were more pronounced 7 days later (Figure 4I-N). At the same time, we detected the expression of genes related to osteogenesis, mainly Runx2, BMP-2, OCN and OPN. PCR results indicated
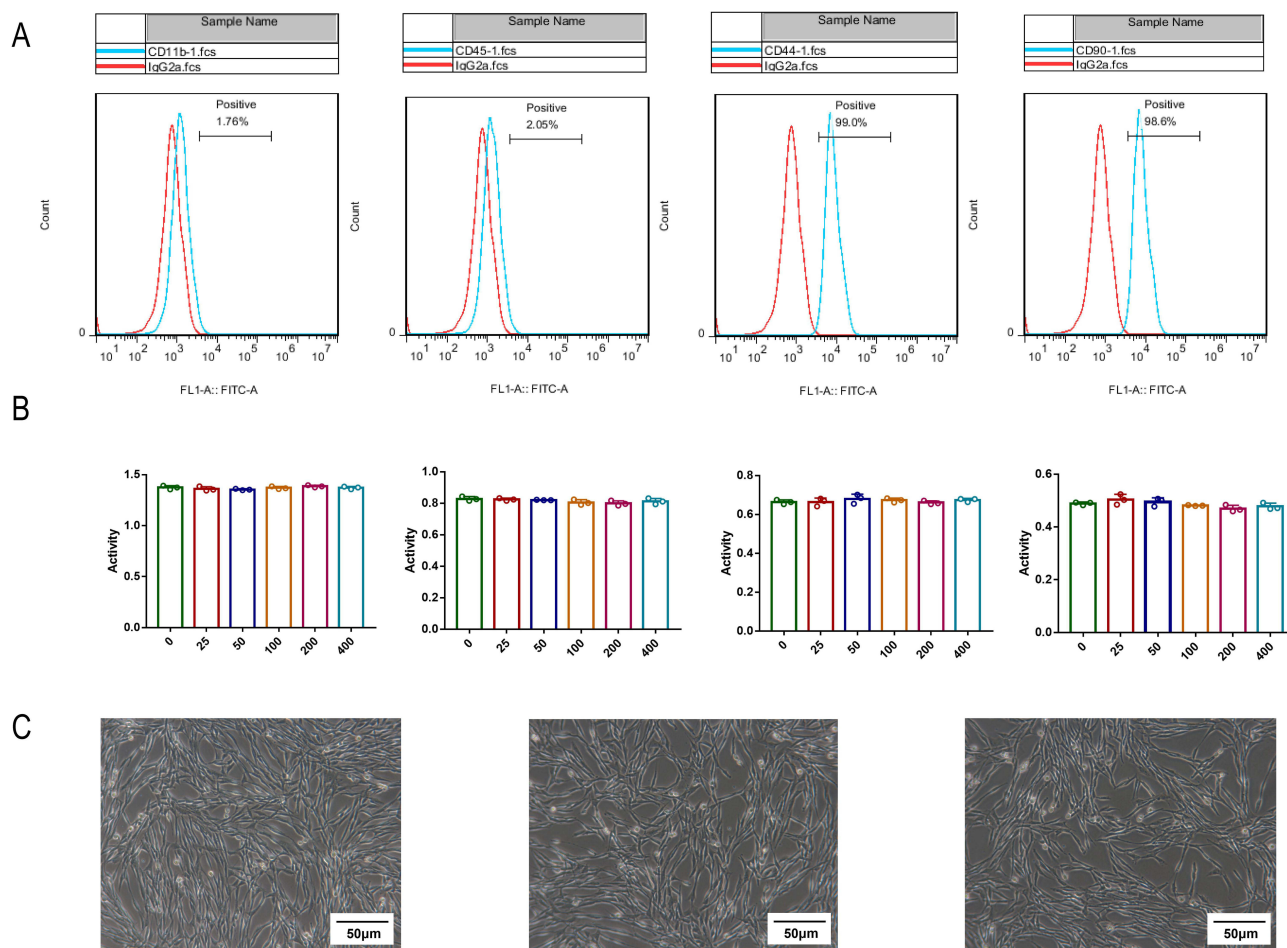
Figure 3 Determination of material safety in vivo. (**A**) Effects on vital organs in black and experimental group, from left to right are heart, liver, kidney, spleen and lung. (**B**) Liver and kidney function and blood routine after surgery for a week, from left to right are hemoglobin, white blood cells, platelets, urea nitrogen, AST and ALT. (**C**) Liver and kidney function and blood routine after surgery for a week, from left to right are hemoglobin, white blood cells, platelets, urea nitrogen, AST and ALT.

that the expression levels of the above four genes were significantly increased (Figure 4O-R), and we found that BMP-2 and Runx2 were significantly increased. This suggests that the osteogenic mechanism of this material may be closely related to the phosphorylation of Smad.

Sr@Zn@SiO$_2$ Regulated Osteogenesis by Smad1/5/9 Related Targets

After 14 days of osteogenic induction, Western blot was used to determine the expression levels of β-actin and Smad1/5/9 in control group, blank group and material group, and the results showed no significant statistical difference (Figure 5A-D). As for the expression of p-Smad1/5/9, the results indicated that the expression of p-Smad1/5/9 was significantly increased in the material group (Figure 5A-D). The analysis of immunofluorescence staining results in the control group, blank group and material group indicated that the expression of p-Smad1/5/9 was different (Figure 5E-G). This confirmed that the Sr@Zn@SiO$_2$ can activate the target role of p-Smad1/5/9 in the regulation of osteogenesis and thus stimulate the expression of downstream osteogenic genes. We also obtained the same result by using image J software for quantitative analysis of average fluorescence intensity (Figure 5H and I).

Sr@Zn@SiO$_2$ Promoted the Repair of Bone Defect in Rats

The osteogenic effect of the material was confirmed by establishing a rat femur defect model, and the specific process can be found in Figure 6A. The sections of the stained sections were observed under electron microscopy at 4 and 8 weeks after filling the bone defect, respectively. It was found that only a small amount of bone tissue surrounding was visible in
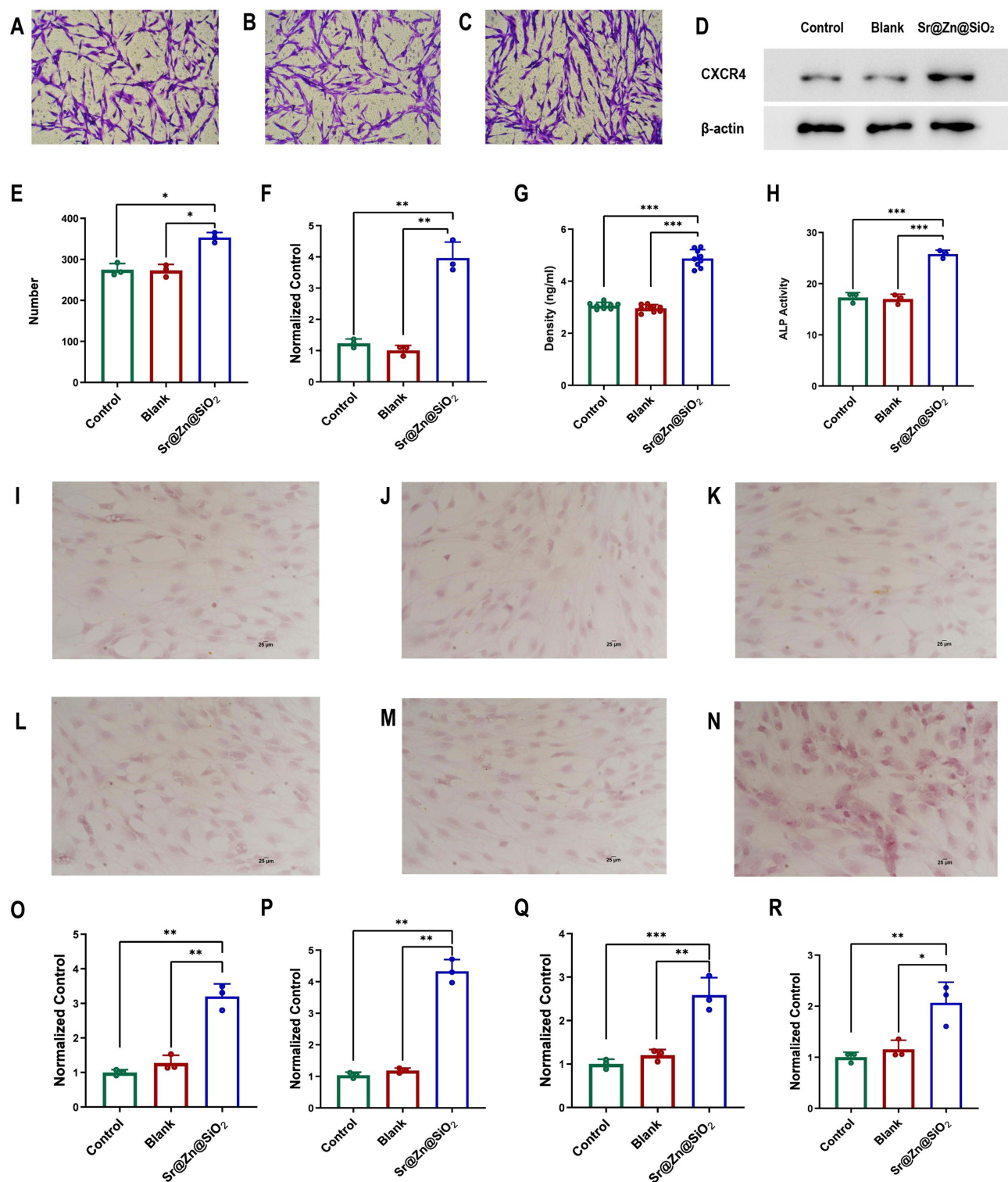
Figure 4 The assessment of Sr@Zn@SiO$_2$ on BMSCs migration and bone formation. (**A-C**) Detailed figures of Transwell migration assay of three groups, the control group, and the blank group. (**D**) The expression of CXCR4 protein in control group, blank group and material group were detected by WB. (**E**) The migration ability of BMSCs. The migration cell counts of control group, the blank group, and the material group. (**F**) The expression of CXCR4 gene in 3 groups were detected by PCR. (**G**) The expression of CXCL12 in control group, blank group and material group was detected by Elisa. (**H**) ALP relative activity analysis of control group, blank group and material group. (**I-K**) The alizarin red staining results of control group, blank group and material group a day after the model was built. (**L-N**) The alizarin red staining results of control group, blank group and material group 7 days after the model was built. (**O-R**) PCR detection of Runx2, BMP-2, OCN and OPN gene expression in control, blank and material groups. (*P <0.05, **P < 0.01, ***P < 0.001).
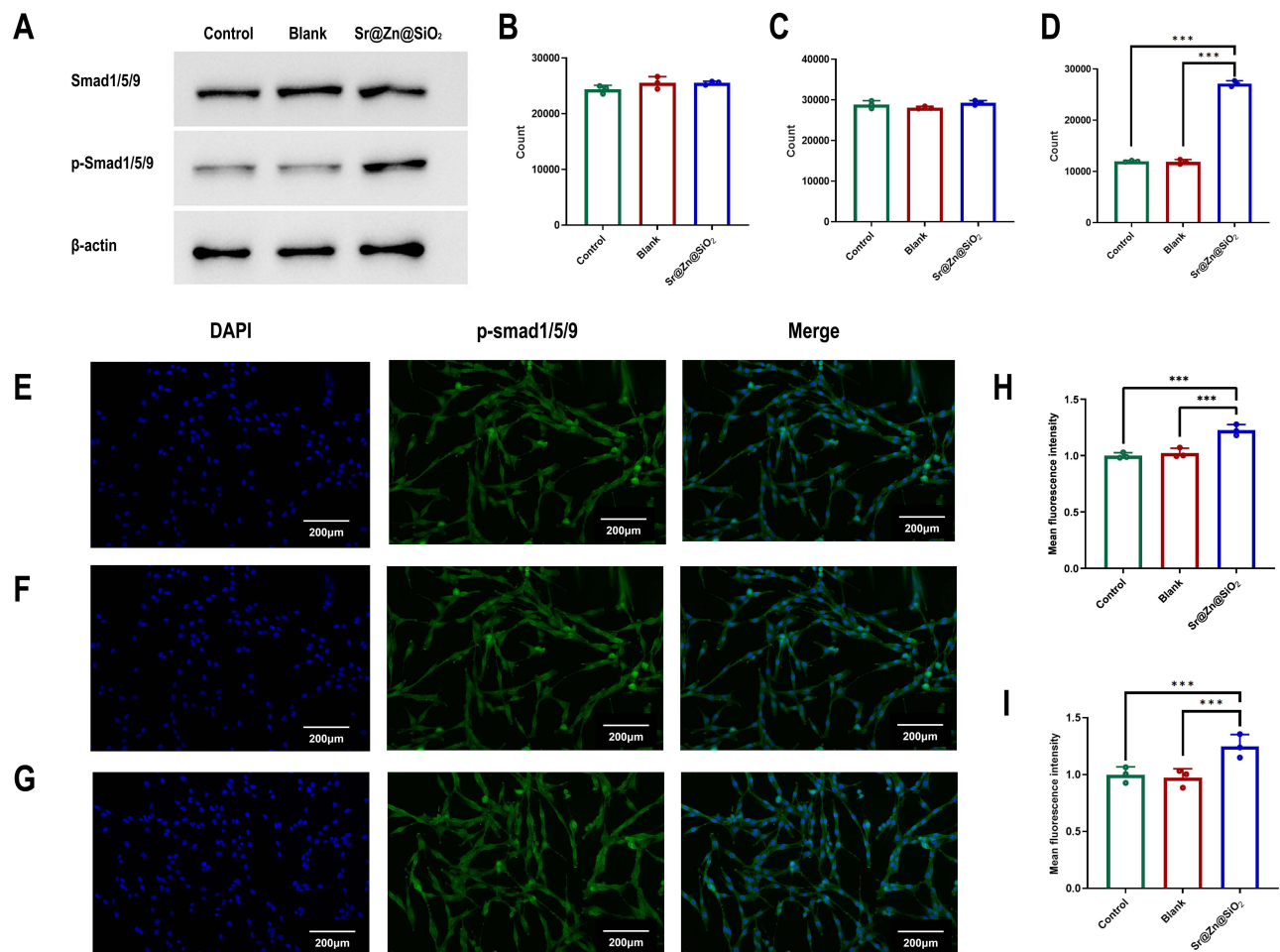
Figure 5 Smad1/5/9 and p-Smad1/5/9 protein expression levels. (**A**) Western blot strip plots of control group, blank group and material group. (**B-D**) Quantitative analysis of Western blot results of control group, blank group and material group. (**E-G**) Immunofluorescence images of three groups. (**H-I**) Quantitative analysis of the average fluorescence intensity of 3 groups. (***$P < 0.001$).

the blank and control groups, while a larger amount of new bone tissue was seen in the material group (Figure 6B-D), and this phenomenon became more obvious at 8 weeks (Figure 6E-G). The results of Micro-CT indicated that bone formation in the material group was significantly better than that in the other two groups after four weeks (Figure 6H-J), and was even more obvious after eight weeks (Figure 6K-M). After quantitative analysis of osteogenesis indicators, we found that BMD, Tb. N, BV/TV and Tb. Th, the material group had more advantages, no matter at 4 weeks or 8 weeks. While in terms of Po. V, the material group had less advantages than the other two groups (Figure 6N-W).

Discussion

Bone marrow mesenchymal stem cells are affected by various factors in the process of osteogenic differentiation, among which the temperature, humidity and pH of the environment play an important role.[27] In addition to the most basic environment, BMP-2 and calcium ion are clearly capable of osteogenesis.[28] Some targeted biofilms can carry some osteogenic drugs to promote the differentiation of bone marrow mesenchymal stem cells,[29] and it is worth noting that some trace elements also play a huge role in the achievement process.[30]

Many metal elements are required in the process of bone repair, Sr, as an important element in bones, is extremely important. The drug strontium ranelate has been widely used in the treatment of osteoporotic fractures in menopausal women, and bone ceramics incorporated with rhBMP-2 and Sr also have osteogenic effects.[31] Similarly, studies have shown that the addition of strontium improves the bone regeneration ability of mesoporous bioactive glasses.[32] The above studies have confirmed that strontium has a clear osteogenic effect, and recent studies have used SiO_2 as a carrier
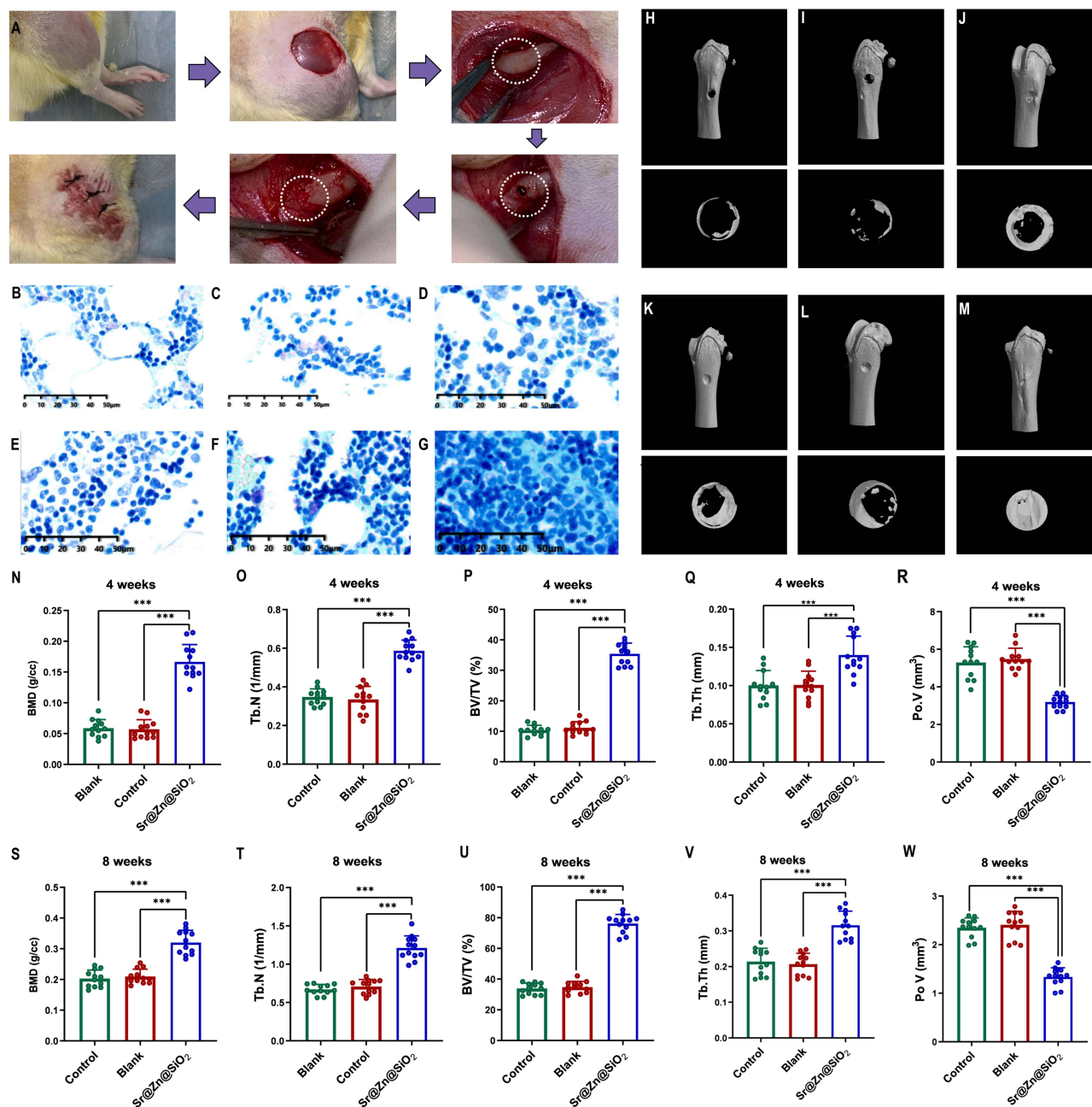
Figure 6 Construction of bone defect model and determination of bone repair in rats. (**A**) The process of Constructing a bone defect model, which including steps such as exposure, drilling, filling, and stitching. (**B-D**) Toluidine blue staining of rat femur after four weeks of material filling about control group, blank group and material group. (**E-G**) Toluidine blue staining of rat femur after eight weeks of material filling about control group, blank group and material group. (**H-J**) Micro-CT image of bone defect repair after four weeks of material filling about three groups. (**K-M**) Micro-CT image of bone defect repair after eight weeks of material filling about three groups. (**N-R**) Determination of the correlative indexes of bone repair after eight weeks of material filling about three groups. (**S-W**) Determination of correlative indexes of bone repair after 4 weeks of material filling about three groups. (***P < 0.001).

for metal elements, suggesting that $Mg@Sr@SiO_2$ also has osteogenic ability.[33] The combination of Zn and SiO_2 appeared earlier and has clear angiogenic and osteogenic effects in the body.[34] Sr—the primary component in osteoporosis medications—has been shown to stimulate osteogenesis through multiple pathways. Concurrently, Zn has been implicated in bone formation, with studies pointing to its regulatory effects on alkaline phosphatase activity and its role in BMSCs-mediated osteogenic differentiation.[13]

And previous research results have confirmed strontium and zinc have osteogenic effects,[35] in our study, we performed osteogenesis studies using both materials in vivo and in vitro and achieved significant osteogenesis results.

Based on the slow-release properties of silica nanocomposite implant,[36] we synthesized $Sr@Zn@SiO_2$ nanocomposite implant.

After passing the element distribution and detection as well as TEM technique, the safety of this material was verified by CCK-8 experiment and co-culture with cells. It lays a foundation for the following animal and cell experimental research. In recent years, BMSCs have been widely concerned and applied in the process of bone repair.[37] The main reason is that these cells have abundant sources, strong proliferation ability, low culture requirement and stable expression.[38,39] They have strong differentiation potential and are also key cells in the process of human bone formation. At present, it is considered as an ideal seed cell for the treatment of bone defects. Based on this, we isolated and identified BMSCs. Although there is no specific surface marker on BMSCs surface,[40] a variety of molecules expressed on BMSCs surface provide methods for identification, such as CD29, CD49, CD54, CD71, CD106, CD166 and others, all of these are expressed on BMSCs. Among them, CD44 and CD90 are the most specific. In addition, CD14, CD31, CD34 and CD35 were not expressed on the cell surface, among which CD45 and CD11b were the most specific.[40] In this study, we identified these specific molecules.

In the process of osteogenesis, the migration and differentiation of BMSCs are particularly important, in which good migration ability can promote the aggregation of BMSCs to the defect, while strong differentiation function can play a regenerative function in the bone defect. The two functions cooperate with each other and work together to achieve the purpose of promoting bone healing. Based on this, for the detection of cell migration ability, we chose the traditional Transwell migration assay to evaluate the migration ability of bone marrow mesenchymal stem cells. This method is currently a highly reliable method and has been applied in the research of cell invasion and metastasis ability.[41] The results suggest that this material plays a role in the migration of BMSCs. At the same time, based on the appearance of the characterization of material promoting migration, we explored its internal mechanism. CXCL12, as a member of the chemokine family, has a strong role in regulating cell function,[42,43] and CXCR4, as the only receptor of CXCL12, can combine with CXCL12 to form a signal axis. It can increase the number of hematopoietic stem cells in bone marrow, and improve the migration ability of BMSCs.[21] We detected the expressions of CXCL12 and CXCR4 in the three groups by various biochemical methods, which explained the mechanism of the positive effect of $Sr@Zn@SiO_2$ on the early migration of BMSCs.

In the differentiation function of BMSCs, we found that this material had a strong effect on bone formation, and the amount of calcium is particularly important during bone formation, and in the process of bone formation induction, calcium ions will be deposited in the form of calcium salts, and alizarin red staining can precisely stain calcium salts red.[44] Similarly, as a landmark enzyme in osteogenesis, alkaline phosphatase mainly promotes calcium mineralization, and its increased activity also lays the foundation for improving osteogenesis.[45] Our results confirmed that there were significant statistical differences in the results of alizarin red staining and alkaline phosphatase staining among the three groups.

Based on the results of alizarin red staining and alkaline phosphatase staining, we also attempted to find its internal mechanism. First, we detected some classic osteogenic genes, among which BMP is a member of TGF-β family, it can stimulate the maturation of mesenchymal stem progenitor cells into osteoblasts,[46] and runt-related transcription factor 2 (Runx2), encoded by Runx2 gene, is a key transcription factor regulating osteoblast differentiation.[47] OCN and OSX are generally considered to be typical osteogenic markers[48] and play an important role in regulating bone matrix mineralization. Based on the theory of previous studies, we measured the expression of the above four genes, and found that the reason for the differences in osteogenesis was indeed due to changes in osteogenic genes. Among the genes selected for detection, BMP-2, as the upstream gene of Runx2, can regulate the expression of Runx2 and OSX as well as downstream genes through phosphorylation of Smad.[49] This suggests that the phosphorylation of Smad is the core mechanism of osteogenesis in this material. Based on this, we further explored the intrinsic core target Smad1/5/9 of osteogenesis in this material.

BMP can play a regulatory and induction role through two types of classical and non-classical Smad signaling targets. In previous studies, Smad1/5/9 belongs to the BMP-activated Smad family, and BMP can activate Smad1/5/9 to phosphorylate to form p-Smad1/5/9.[5] p-Smad1/5/9 can form Smad4 into a complex, and the level of the complex will directly regulate the expression of downstream transcription factors, such as the most classic Runx2 and OSX osteogenic

genes.[50] Therefore, Smad1/5/9, as a key target of osteogenesis, is extremely important for the differentiation of BMSCs. Based on the above theories, we analyzed the expression of p-Smad1/5/9 by Western blot and immunofluorescence staining, and confirmed the role of this target in the osteogenesis process of this material. Therefore, we have reason to believe that Sr@Zn@SiO$_2$ nanocomposite can achieve the purpose of bone repair by regulating this target.

After the completion of the in vitro experiment, we constructed the bone defect model of the rat femur and filled the bone defect with materials. By comparing the bone tissue section staining of the three groups, the bone defect reconstructed by Micro-CT and BMD, Tb.N, BV/TV, Tb.Th. We confirmed the bone formation ability of the material in vivo. Both in vivo and in vitro experiments, the Sr@Zn@SiO$_2$ nanocomposite has played a specific role in osteogenesis. In this study, we explored the mechanisms involved in cell migration and cell proliferation and differentiation.

In the inflammatory microenvironment caused by trauma, osteogenesis is often more difficult to occur. Zn ions have a strong anti-inflammatory effect and can increase the expression of osteogenic related proteins in mouse osteoblasts in the inflammatory microenvironment. Silicon, as a carrier, can also exhibit stable sustained release and stability in inflammatory environments. Studies have shown that porous silicon-based nanomedicine has clear potential in effectively controlling the treatment of rheumatoid arthritis.[51]

Based on the conclusion of biological verification and mechanism exploration, the material has broad application prospects. Firstly, for patients with fractures, appropriate addition of this material in the process of internal fixation and implantation can not only prevent the occurrence of surgical infection, but also speed up bone repair, which is good news for patients with fractures. At the same time, the treatment of some patients with bone defects in special circumstances will be equally effective. Metal Sr, as the core element of the treatment of osteoporosis, is the main component of the drug strontium ranelate, so the material will have a more far-reaching significance for the bone defect of osteoporosis patients,[52] and for patients with osteomyelitis, the zinc element in the material will also play an antibacterial role.[53] And the osteogenic potential of this material in future inflammatory environments is also promising. The bioactive material may also have some potential in angiogenesis, and the Zn element will play a greater role, which needs our follow-up verification, this material in the future application potential will be greater. Although the material has a broad future application prospect, similarly, the research and application of other nanomaterials also have certain value.[54–56]

Conclusion

In this study, Sr@Zn@SiO$_2$ nanocomposite implant was synthesized and verified for the first time. After safety testing, we found that porous Sr@Zn@SiO$_2$ nanocomposite can promote the migration of BMSCs by activating the CXCL12/ CXCR4 axis. At the same time, the phosphorylation of Smad/1/5/9 can be activated by BMP-2 to promote the expression of Runx-2 and OSX downstream, thus promoting the differentiation of BMSCs. Finally, we established a bone defect model in rats, and evaluated the effect of the material on new bone mass by qualitative and quantitative analysis, and proved that Sr@Zn@SiO$_2$ can accelerate the process of bone defect repair in vivo. The emergence of this new bioactive porous composite implant has certain enlightening effects on the clinical treatment of bone defects. We hope that it can be applied to clinical patients as soon as possible to promote the progress of bone defect treatment.

Abbreviations

SiO$_2$, Silicon Dioxide; Sr, Strontium; Zn, Zinc; BMSCs, Bone Marrow Stromal Cells; BMP-2, Bone Morphogenetic Protein; Runx2, Runt-related transcription factor 2; OCN, Osteocalci; OSX, Osterix; TEM, Transmission Electron Microscopy; CTAB, Cetyl Trimethyl Ammonium Bromide; TEOS, tetraethyl orthosilicate;PVP, Polyvinylpyrrolidone; PBS, phosphate buffer saline; WB, Western Blot; ALP, Alkaline phosphatase; TEOS, Tetraethyl orthosilicate; PCR, Polymerase Chain Reaction;Elisa, Enzyme linked immunosorbent assay;ALP, Alkaline phosphatase; BMD, Bone mineral density; Tb. N, Number of trabeculae; BV/TV, Bone volume fraction; Tb. Th, Trabecular Thickness.

Author Contributions

All authors made a significant contribution to the work reported, whether that is in the conception, study design, execution, acquisition of data, analysis and interpretation, or in all these areas; took part in drafting, revising or critically

reviewing the article; gave final approval of the version to be published; have agreed on the journal to which the article has been submitted; and agree to be accountable for all aspects of the work.

Funding

Disclosure

The authors report no conflicts of interest in this work.

References

1. Dimitriou R, Jones E, McGonagle D, Giannoudis PV. Bone regeneration: current concepts and future directions. *BMC Med*. 2011;9:66. doi:10.1186/1741-7015-9-66
2. Hadjiargyrou M, O'Keefe RJ. The convergence of fracture repair and stem cells: interplay of genes, aging, environmental factors and disease. *J Bone Mineral Res*. 2014;29(11):2307–2322. doi:10.1002/jbmr.2373
3. Ning K, Liu S, Yang B, et al. Update on the effects of energy metabolism in bone marrow mesenchymal stem cells differentiation. *Mol Metabol*. 2022;58:101450. doi:10.1016/j.molmet.2022.101450
4. Fu X, Liu G, Halim A, Ju Y, Luo Q, Song AG. Mesenchymal stem cell migration and tissue repair. *Cells*. 2019;8(8):784. doi:10.3390/cells8080784
5. Li C, Wang Q, Gu X, et al. Porous Se@SiO(2) nanocomposite promotes migration and osteogenic differentiation of rat bone marrow mesenchymal stem cell to accelerate bone fracture healing in a rat model. *Int J Nanomed*. 2019;14:3845–3860. doi:10.2147/IJN.S202741
6. Liu Y, Zhu J, Xu L, Wang B, Lin W, Luo Y. Copper regulation of immune response and potential implications for treating orthopedic disorders. *Front Mol Biosci*. 2022;9:1065265. doi:10.3389/fmolb.2022.1065265
7. Mutlu N, Liverani L, Kurtuldu F, Galusek D, Boccaccini AR. Zinc improves antibacterial, anti-inflammatory and cell motility activity of chitosan for wound healing applications. *Int J Biol Macromol*. 2022;213:845–857. doi:10.1016/j.ijbiomac.2022.05.199
8. Hochvaldová L, Panáček D, Válková L, et al. Restoration of antibacterial activity of inactive antibiotics via combined treatment with a cyanographene/Ag nanohybrid. *Sci Rep*. 2022;12(1):5222. doi:10.1038/s41598-022-09294-7
9. Deeks ED, Dhillon S. Strontium ranelate: a review of its use in the treatment of postmenopausal osteoporosis. *Drugs*. 2010;70(6):733–759. doi:10.2165/10481900-000000000-00000
10. Zhang W, Huang D, Zhao F, et al. Synergistic effect of strontium and silicon in strontium-substituted sub-micron bioactive glass for enhanced osteogenesis. *Mater Sci Eng C Mater Biol Appl*. 2018;89:245–255. doi:10.1016/j.msec.2018.04.012
11. Dong J, Lin P, Putra NE, et al. Extrusion-based additive manufacturing of Mg-Zn/bioceramic composite scaffolds. *Acta Biomater*. 2022;151:628–646. doi:10.1016/j.actbio.2022.08.002
12. Jin G, Qin H, Cao H, et al. Synergistic effects of dual Zn/Ag ion implantation in osteogenic activity and antibacterial ability of titanium. *Biomaterials*. 2014;35(27):7699–7713. doi:10.1016/j.biomaterials.2014.05.074
13. Melnik EV, Shkarina SN, Ivlev SI, et al. In vitro degradation behaviour of hybrid electrospun scaffolds of polycaprolactone and strontium-containing hydroxyapatite microparticles. *Polym Degrad Stab*. 2019;167:21–32. doi:10.1016/j.polymdegradstab.2019.06.017
14. Conte R, Valentino A, Romano S, Margarucci S, Petillo O, Calarco A. Stimuli-responsive nanocomposite hydrogels for oral diseases. *Gels*. 2024;10(7).
15. Li X, Wang Q, Deng G, et al. Porous Se@SiO2 nanospheres attenuate cisplatin-induced acute kidney injury via activation of Sirt1. *Toxicol Appl Pharmacol*. 2019;380:114704. doi:10.1016/j.taap.2019.114704
16. Maser E, Schulz M, Sauer UG, et al. In vitro and in vivo genotoxicity investigations of differently sized amorphous SiO2 nanomaterials. *Mutat Res*. 2015;794:57–74. doi:10.1016/j.mrgentox.2015.10.005
17. Gao T, Aro HT, Ylänen H, Vuorio E. Silica-based bioactive glasses modulate expression of bone morphogenetic protein-2 mRNA in Saos-2 osteoblasts in vitro. *Biomaterials*. 2001;22(12):1475–1483. doi:10.1016/S0142-9612(00)00288-X
18. Hu Y, Wang Y, Feng Q, et al. Zn-Sr-sintered true bone ceramics enhance bone repair and regeneration. *Biomater Sci*. 2023;11(10):3486–3501. doi:10.1039/D3BM00030C
19. Cui Y, Cheng M, Han M, Zhang R, Wang X. Characterization and release kinetics study of potato starch nanocomposite films containing mesoporous nano-silica incorporated with Thyme essential oil. *Int J Biol Macromol*. 2021;184:566–573. doi:10.1016/j.ijbiomac.2021.06.134
20. Só BB, Silveira FM, Llantada GS, et al. Effects of osteoporosis on alveolar bone repair after tooth extraction: a systematic review of preclinical studies. *Arch Oral Biol*. 2021;125:105054. doi:10.1016/j.archoralbio.2021.105054
21. Moll NM, Ransohoff RM. CXCL12 and CXCR4 in bone marrow physiology. *Exp Rev Hematol*. 2010;3(3):315–322. doi:10.1586/ehm.10.16
22. Agas D, Sabbieti MG, Marchetti L, Xiao L, Hurley MM. FGF-2 enhances Runx-2/Smads nuclear localization in BMP-2 canonical signaling in osteoblasts. *J Cell Physiol*. 2013;228(11):2149–2158. doi:10.1002/jcp.24382
23. Farshdousti Hagh M, Noruzinia M, Mortazavi Y, et al. Different methylation patterns of RUNX2, OSX, DLX5 and BSP in osteoblastic differentiation of mesenchymal stem cells. *Cell J*. 2015;17(1):71–82. doi:10.22074/cellj.2015.513
24. Niu T, Shi X, Liu X, Wang H, Liu K, Xu Y. Porous Se@SiO(2) nanospheres alleviate diabetic retinopathy by inhibiting excess lipid peroxidation and inflammation. *Mol med*. 2024;30(1):24. doi:10.1186/s10020-024-00785-z
25. Yang YX, Liu MS, Liu XJ, et al. Porous Se@SiO(2) nanoparticles improve oxidative injury to promote muscle regeneration via modulating mitochondria. *Nanomedicine*. 2022;17(21):1547–1565. doi:10.2217/nnm-2022-0173
26. Kilkenny C, Browne WJ, Cuthill IC, Emerson M, Altman DG. Improving bioscience research reporting: the ARRIVE guidelines for reporting animal research. *PLoS Biol*. 2010;8(6):e1000412. doi:10.1371/journal.pbio.1000412

27. Pal R, Hanwate M, Totey SM. Effect of holding time, temperature and different parenteral solutions on viability and functionality of adult bone marrow-derived mesenchymal stem cells before transplantation. *J Tissue Eng Regener Med*. 2008;2(7):436–444. doi:10.1002/term.109

28. Aquino-Martínez R, Artigas N, Gámez B, Rosa JL, Ventura F. Extracellular calcium promotes bone formation from bone marrow mesenchymal stem cells by amplifying the effects of BMP-2 on SMAD signalling. *PLoS One*. 2017;12(5):e0178158. doi:10.1371/journal.pone.0178158

29. Uzieliene I, Bironaite D, Bagdonas E, et al. The effects of mechanical load on chondrogenic responses of bone marrow mesenchymal stem cells and chondrocytes encapsulated in chondroitin sulfate-based hydrogel. *Int J Mol Sci*. 2023;24(3):2915. doi:10.3390/ijms24032915

30. Salamanna F, Giavaresi G, Contartese D, et al. Effect of strontium substituted ß-TCP associated to mesenchymal stem cells from bone marrow and adipose tissue on spinal fusion in healthy and ovariectomized rat. *J Cell Physiol*. 2019;234(11):20046–20056. doi:10.1002/jcp.28601

31. Zhang C, Xu G, Han L, Hu X, Zhao Y, Li Z. Bone induction and defect repair by true bone ceramics incorporated with rhBMP-2 and Sr. *J Mater Sci Mater Med*. 2021;32(9):107. doi:10.1007/s10856-021-06587-7

32. Fiorilli S, Molino G, Pontremoli C, et al. The incorporation of strontium to improve bone-regeneration ability of mesoporous bioactive glasses. *Materials*. 2018;11(5):678.

33. Li C, Yan T, Lou Z, et al. Characterization and in vitro assessment of three-dimensional extrusion Mg-Sr codoped SiO(2)-complexed porous microhydroxyapatite whisker scaffolds for biomedical engineering. *Biomed Eng Online*. 2021;20(1):116. doi:10.1186/s12938-021-00953-w

34. Fielding G, Bose S. SiO2 and ZnO dopants in three-dimensionally printed tricalcium phosphate bone tissue engineering scaffolds enhance osteogenesis and angiogenesis in vivo. *Acta Biomater*. 2013;9(11):9137–9148.

35. Place ES, Rojo L, Gentleman E, Sardinha JP, Stevens MM. Strontium- and zinc-alginate hydrogels for bone tissue engineering. *Tissue Eng Part A*. 2011;17(21–22):2713–2722. doi:10.1089/ten.tea.2011.0059

36. Castillo RR, Vallet-Regí M. Functional mesoporous silica nanocomposites: biomedical applications and biosafety. *Int J Mol Sci*. 2019;20(4):929. doi:10.3390/ijms20040929

37. Mobasheri A, Kalamegam G, Musumeci G, Batt ME. Chondrocyte and mesenchymal stem cell-based therapies for cartilage repair in osteoarthritis and related orthopaedic conditions. *Maturitas*. 2014;78(3):188–198. doi:10.1016/j.maturitas.2014.04.017

38. Qi Y, Yan W. Mesenchymal stem cell sheet encapsulated cartilage debris provides great potential for cartilage defects repair in osteoarthritis. *Med Hypotheses*. 2012;79(3):420–421. doi:10.1016/j.mehy.2012.05.024

39. Pajarinen J, Lin T, Gibon E, et al. Mesenchymal stem cell-macrophage crosstalk and bone healing. *Biomaterials*. 2019;196:80–89. doi:10.1016/j.biomaterials.2017.12.025

40. Wang LS, Wang H, Zhang QL, Yang ZJ, Kong FX, Wu CT. Hepatocyte growth factor gene therapy for ischemic diseases. *Human Gene Ther*. 2018;29(4):413–423. doi:10.1089/hum.2017.217

41. Omar Zaki SS, Kanesan L, Leong MYD, Vidyadaran S. The influence of serum-supplemented culture media in a transwell migration assay. *Cell Biol Int*. 2019;43(10):1201–1204. doi:10.1002/cbin.11122

42. Janssens R, Struyf S, Proost P. Pathological roles of the homeostatic chemokine CXCL12. *Cytokine Growth Factor Rev*. 2018;44:51–68. doi:10.1016/j.cytogfr.2018.10.004

43. Nagasawa T. CXC chemokine ligand 12 (CXCL12) and its receptor CXCR4. *J mol med*. 2014;92(5):433–439. doi:10.1007/s00109-014-1123-8

44. Ding J, Yan R, Wang L, et al. Using alizarin red staining to detect chemically induced bone loss in zebrafish larvae. *J Visualized Exp*. 2021; 178. doi:10.3791/63251-v

45. Nizet A, Cavalier E, Stenvinkel P, Haarhaus M, Magnusson P. Bone alkaline phosphatase: an important biomarker in chronic kidney disease - mineral and bone disorder. *Int J Clin Chem*. 2020;501:198–206. doi:10.1016/j.cca.2019.11.012

46. Chen G, Deng C, Li YP. TGF-β and BMP signaling in osteoblast differentiation and bone formation. *Int J Bio Sci*. 2012;8(2):272–288. doi:10.7150/ijbs.2929

47. Komori T. Runx2, an inducer of osteoblast and chondrocyte differentiation. *Histochem Cell Biol*. 2018;149(4):313–323. doi:10.1007/s00418-018-1640-6

48. Song ZH, Xie W, Zhu SY, Pan JJ, Zhou LY, He CQ. Effects of PEMFs on Osx, Ocn, TRAP, and CTSK gene expression in postmenopausal osteoporosis model mice. *Int J Clin Exp Pathol*. 2018;11(3):1784–1790.

49. Li J, Xiong S, Ding L, et al. The mechanism research of non-Smad dependent TAK1 signaling pathway in the treatment of bone defects by recombination BMP-2-loaded hollow hydroxyapatite microspheres/chitosan composite. *J Mater Sci Mater Med*. 2019;30(12):130. doi:10.1007/s10856-019-6340-9

50. Yan CP, Wang XK, Jiang K, et al. β-Ecdysterone enhanced bone regeneration through the BMP-2/SMAD/RUNX2/osterix signaling pathway. *Front Cell Develop Biol*. 2022;10:883228. doi:10.3389/fcell.2022.883228

51. Jeong M, Jung Y, Yoon J, et al. Porous silicon-based nanomedicine for simultaneous management of joint inflammation and bone erosion in rheumatoid arthritis. *ACS nano*. 2022;16(10):16118–16132. doi:10.1021/acsnano.2c04491

52. Strontium ranelate for osteoporosis? *Drug Ther Bull*. 2006;44(4):29–32. doi:10.1136/dtb.2006.44429

53. Jia B, Zhang Z, Zhuang Y, et al. High-strength biodegradable zinc alloy implants with antibacterial and osteogenic properties for the treatment of MRSA-induced rat osteomyelitis. *Biomaterials*. 2022;287:121663. doi:10.1016/j.biomaterials.2022.121663

54. Kim HS, Lee JH, Mandakhbayar N, et al. Therapeutic tissue regenerative nanohybrids self-assembled from bioactive inorganic core / chitosan shell nanounits. *Biomaterials*. 2021;274:120857. doi:10.1016/j.biomaterials.2021.120857

55. Patel KD, Buitrago JO, Parthiban SP, et al. Combined effects of nanoroughness and ions produced by electrodeposition of mesoporous bioglass nanoparticle for bone regeneration. *ACS Appl Bio Mater*. 2019;2(11):5190–5203. doi:10.1021/acsabm.9b00859

56. Kang MS, Lee NH, Singh RK, et al. Nanocements produced from mesoporous bioactive glass nanoparticles. *Biomaterials*. 2018;162:183–199. doi:10.1016/j.biomaterials.2018.02.005